

-

**EMERGENCE, COMPLEXITE, UNIVERSALITE des SYSTEMES à N CORPS:  
NOYAUX, ATOMES FROIDS, AGREGATS METALLIQUES, MOLECULES, ...**

**P. Schuck**

IPNO

## CONTENT

**Nuclear Mean Field:** dead end.

**Inclusion of quantal fluctuations and more correlations**

**Second RPA; Coupled Cluster; TDDM.**

**Overlap with Chemistry**

**Overlap with Cold Atoms**

**Overlap with small metallic clusters**

**Conclusions**

# MEAN FIELD APPROACH

About 250 Skyrme forces and nuclear EDF's !!

Stone et al

PHYSICAL REVIEW C **85**, 035201 (2012)

## Skyrme interaction and nuclear matter constraints

M. Dutra,<sup>\*</sup> O. Lourenço,<sup>\*</sup> J. S. Sá Martins, and A. Delfino

*Instituto de Física–Universidade Federal Fluminense, Avenida Litorânea s/n, 24210-150 Boa Viagem, Niterói RJ, Brazil*

J. R. Stone

*Oxford Physics, University of Oxford, Oxford OX1 3PU, United Kingdom and  
Department of Physics and Astronomy, University of Tennessee, Knoxville, Tennessee 37996, USA*

P. D. Stevenson

*Department of Physics, University of Surrey, Guildford GU2 7XH, United Kingdom*

(Received 16 November 2011; revised manuscript received 27 January 2012; published 5 March 2012)

This paper presents a detailed assessment of the ability of the 240 Skyrme interaction parameter sets in the literature to satisfy a series of criteria derived from macroscopic properties of nuclear matter in the vicinity of nuclear saturation density at zero temperature and their density dependence, derived by the liquid-drop model, in experiments with giant resonances and heavy-ion collisions. The objective is to identify those parametrizations which best satisfy the current understanding of the physics of nuclear matter over a wide range of applications. Out of the 240 models, only 16 are shown to satisfy all these constraints. Additional, more microscopic, constraints on the density dependence of the neutron and proton effective mass  $\beta$ -equilibrium matter, Landau parameters of symmetric and pure neutron nuclear matter, and observational data on high- and low-mass cold neutron stars further reduce this number to 5, a very small group of recommended Skyrme parametrizations to be used in future applications of the Skyrme interaction of nuclear-matter-related observables. Full information on partial fulfillment of individual constraints by all Skyrme models considered is given. The results are discussed in terms of the physical interpretation of the Skyrme interaction and the validity of its use in mean-field models. Future work on application of the Skyrme forces, selected on the basis of variables of nuclear matter, in the Hartree-Fock calculation of properties of finite nuclei, is outlined.

# In any case quantal fluctuations have to be included: Tselyaev:

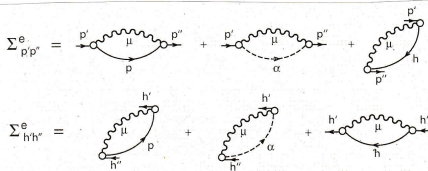


FIG. 1. Particle  $\Sigma_{p'p''}^e$  and hole  $\Sigma_{h'h''}^e$  components of the relativistic mass operator in the graphical representation. Solid and dashed lines with arrows denote one-body propagators for particle (p), hole (h), and antiparticle ( $\alpha$ ) states. Wavy lines denote phonon ( $\mu$ ) propagators, empty circles are the particle-phonon coupling amplitudes  $\gamma^\mu$ .

064308-4

E. LITVINOVA, P. RING, AND V. TSELYAEV

PHYSICAL REVIEW C 75, 064308 (2007)

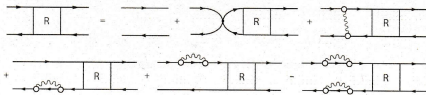
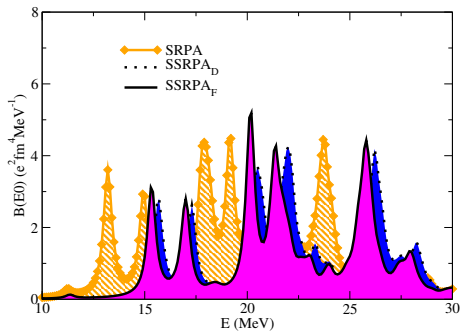


FIG. 2. Bethe-Salpeter equation for p-h response function  $R$  in graphical representation. Details are given in Fig. 1; small black circle means the static part of the residual p-h interaction (20).

New parameter fit!! **Very large program!!**



Second RPA with substraction; monopole spectrum, M. Grasso et al.

## GW approach (electron gas)

$$\Sigma(1,2) = iG(1,2)W(1,2)$$

$W$  = screened Coulomb exchange with RPA:

$$W = v_{\text{Coul}} + v_{\text{Coul}} R v_{\text{Coul}} = \bullet + \text{fish diagram}$$

$R$  = linear response in RPA; some similarity with SRPA.

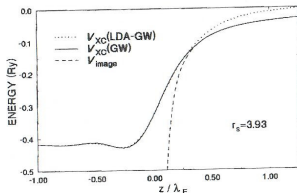


FIG. 14.  $V^{xc}(z)$  at a jellium surface for  $r_s = 3.93$  ( $\lambda_F = 12.9$  a.u.). The solid curve is the solution to equation (151) using the GWA for  $\Sigma$ , and the dotted curve is the corresponding LDA potential. The dashed curve is the image potential  $V^{\text{im}}(z) = -1/4(z - z_0)$ . After Equiluz *et al* (1992).

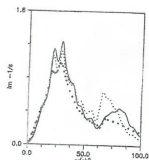


FIG. 15. The imaginary spectra of  $\epsilon$  for  $r_s = 0.25, 0.5, 0.75, 1, 1.5, 2, 3, 4, 6, 8, 10$ . The solid line represents the experimental data from the literature (Binnig, Thoenes, and Hansma (1979)). The dotted line is calculated for the homogeneous electron gas and the dashed line is calculated for the inhomogeneous electron gas at  $r_s = 3.93$ . The curves are calculated with the GW approximation and the RPA approximation (Equiluz *et al* (1992)).

## GW approach to surface of a solid.

Theor Chem Acc (2012) 131:1084  
DOI 10.1007/s00214-011-1084-8

REGULAR ARTICLE

## Electron correlation methods based on the random phase approximation

Henk Eshuis · Jefferson E. Bates · Filipp Furche

Received: 15 June 2011 / Accepted: 16 September 2011 / Published online: 14 January 2012  
© Springer-Verlag 2012

**Table 1** Calculated atomization energies (kcal/mol) compared to experiment

System	PBE	x-only	RPA	RPA+	Expt. <sup>a</sup>
H <sub>2</sub>	105	84	109	110	109
N <sub>2</sub>	244	111	223	223	228
O <sub>2</sub>	144	25	113	111	121
F <sub>2</sub>	53	-43	30	29	38
Ne <sub>2</sub> <sup>b</sup>	0.11	-0.15	0.01	-0.08	0.08 <sup>c</sup>
Si <sub>2</sub>	81	38	70	70	75
HF	142	96	133	132	141
CO	269	170	244	242	259
CO <sub>2</sub>	416	234	364	360	389 <sup>d</sup>
C <sub>2</sub> H <sub>2</sub>	415	291	381	378	405 <sup>d</sup>
H <sub>2</sub> O	234	155	223	222	232 <sup>d</sup>
C <sub>6</sub> H <sub>6</sub> -HF <sup>e</sup>	115	100	112	112	120 ± 1 <sup>f</sup>

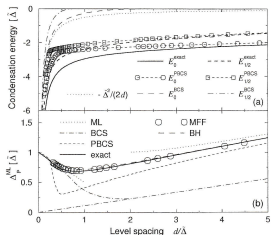


Fig. 14 (a) The even and odd ( $\xi = 0, 1/2$ ) condensation energies  $E_c^{cond}$  of Eq. (52) [in units of  $\Delta$ ], calculated with BCS, PBCS and exact wave functions [35], as functions of  $d/\Delta = 2 \sinh(1/\lambda)/(2n + 2a)$ , for  $\lambda = 0.224$ . For comparison, the dotted line gives the "bulk" result  $E_c^{bulk} = -\Delta^2/(2d)$ . (b) Comparison [35] of the parity parameters  $\Delta_p^{ML}$  [24] of Eq. (53) [in units of  $\Delta$ ] obtained by various authors: ML's analytical result (dotted lines) [ $\Delta(1 - d/2\Delta)$  for  $d \ll \Delta$ , and  $d/2 \log(ed/\Delta)$  for  $d \gg \Delta$ , with  $a = 1.35$  adjusted to give asymptotic agreement with the exact result]; grand-canonical BCS approach (dash-dotted line) [the naive perturbative result  $\frac{1}{2}\lambda d$  is continued to the origin]; PBCS approach (short-dashed line); Richardson's exact solution (solid line); exact diagonalization and scaling by MFF (open circles) and BH (long-dashed line).

## PBCS Ultrasmall metallic clusters

J. van Delft

GENERIC FINITE-SIZE ENHANCEMENT OF PAIRING ...

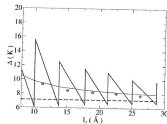


FIG. 1. Dependence of the gap, for the case of a superconducting homogeneous film, on the film thickness  $L$ . The sawtooth line corresponds to a quantum mechanical calculation (Ref. 12), whereas the smooth curve corresponds to formula (8). The horizontal line represents the bulk value  $\Delta_b$  for aluminum. The dots represent the center of gravity of the triangles in which they are lying (a crude way to estimate an average of the quantal results).

Al film

M. FARINE, F. W. J. HEKING, P. SCHÜCK, AND X. VIÑAS

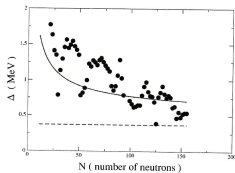


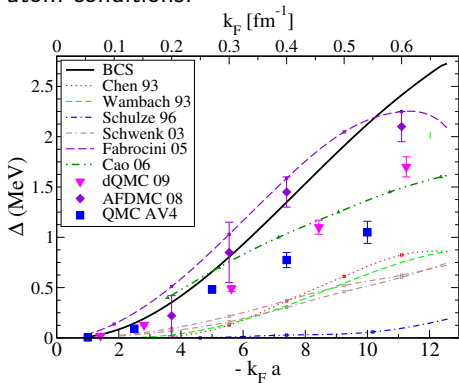
FIG. 2. Average nuclear gaps as a function of neutron number  $N$  along the valley of  $\beta$  stability of the nuclear chart. The experimental points have been taken from Ref. 10. Broken line: the asymptotic value  $\Delta_\infty = 0.37$  MeV to which the full line converges.

nuclei

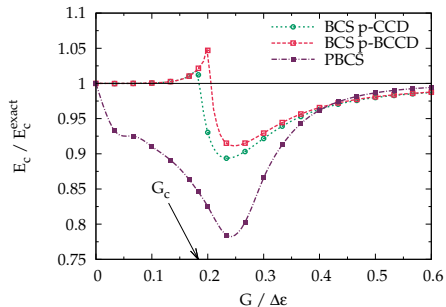
$$\Delta = \Delta_{\text{Bulk}} \left( 1 + \alpha \frac{S}{V} \right)$$

## Pairing in neutron matter

Very long nn s-wave scattering length:  $a_s^{nn} \sim -18$  fm; at low density almost cold atom conditions!



## Coupled Cluster Theory (CCT) Applications in Chemistry and nuclei



False first order phase transition!

# Symmetry broken and restored coupled-cluster theory

## II. Global gauge symmetry and particle number

T. Duguet<sup>1,2,3,\*</sup> and A. Signoracci<sup>4,5,†</sup>

<sup>1</sup>*CEA-Saclay DSM/Irfu/SPhN, F-91191 Gif sur Yvette Cedex, France*

<sup>2</sup>*KU Leuven, Instituut voor Kern- en Stralingsfysica, 3001 Leuven, Belgium*

<sup>3</sup>*National Superconducting Cyclotron Laboratory and Department of Physics and Astronomy,  
Michigan State University, East Lansing, MI 48824, USA*

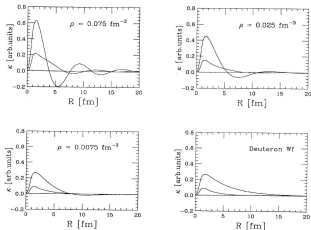
<sup>4</sup>*Department of Physics and Astronomy, University of Tennessee, Knoxville, TN 37996, USA*

<sup>5</sup>*Physics Division, Oak Ridge National Laboratory, Oak Ridge, TN 37831, USA*

(Dated: December 10, 2015)

We have recently extended many-body perturbation theory and coupled-cluster theory performed on top of a Slater determinant breaking rotational symmetry to allow for the restoration of the angular momentum at any truncation order [T. Duguet, J. Phys. G: Nucl. Part. Phys. 42 (2015) 025107]. Following a similar route, we presently extend Bogoliubov many-body perturbation theory and Bogoliubov coupled cluster theory performed on top of a Bogoliubov reference state breaking global gauge symmetry to allow for the restoration of the particle number at any truncation order. Eventually, formalisms can be merged to handle  $SU(2)$  and  $U(1)$  symmetries at the same time. Several further extensions of the newly proposed many-body formalisms can be foreseen in the mid-term future. The long-term goal relates to the ab initio description of near-degenerate finite quantum systems with an open-shell character.

## BEC $\leftrightarrow$ BCS



### Deuterons

FIG. 4. The  $S$  and  $D$  components of the pairing correlation functions in coordinate space for three different values of the baryonic density. The right lower figure displays for comparison the deuteron wave function.

Baldo et al.

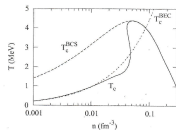


FIG. 7. Superfluid critical temperature as a function of the (total) density. The solid line is the full calculation, while the long dashes correspond to the BCS result. The short dashes show the critical temperature of Bose-Einstein condensation of a deuteron gas.

### Urban, Meng Schuck, PRC

VOLUME 71, NUMBER 19 PHYSICAL REVIEW LETTERS

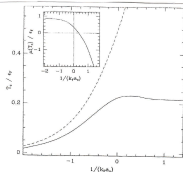
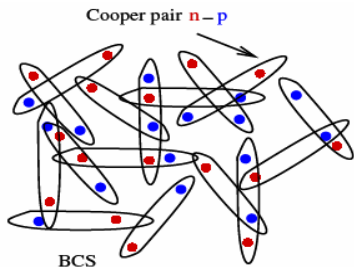
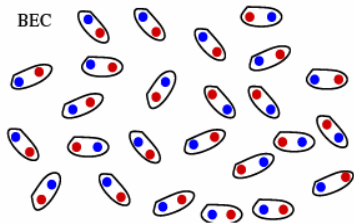


FIG. 1.  $T_c/T_{c0}$  and in the inset  $\rho(T_c)/\rho_0$  as a function of the coupling  $x = 1/k_F a_0$ . The BCS limit corresponds to  $x \rightarrow \infty$  and the Bose regime to  $x \gg 1$ . The dashed line is the saddle point result (see text).

Randeria et al.



Low density :  $\rightleftharpoons$  smooth transition



High Density

$n-p$  Cooper pairs

Strongly overlapping

not Bosons

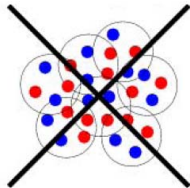


$\alpha$  - Particles  
Only Exist  
in Low Density  
BEC Phase

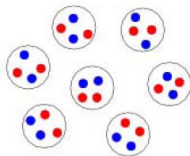
gas of Deuterons

$\sim$  Bosons

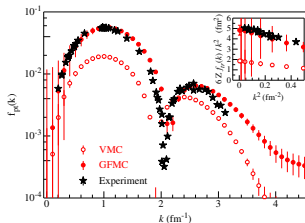
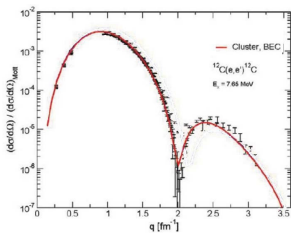
## Quartetting



No BCS phase (dense phase) of  $\alpha$ -particles possible!



Bose-Einstein-Condensation of  $\alpha$ -particles (dilute)



LEFT: **THSR** result; no adjustable parameter;  $\rho = \rho_0/3$

RIGHT: **GFMC** result (R. Wiringa, Pieper, .., RMP); no adjustable parameter

# Self-Consistent RPA $\leftrightarrow$ Time Dependent Density Matrix

Tohyama, P. Sch.

$$i\dot{\rho} = [h^{\text{HF}}, \rho] + vC_2$$

$$i\dot{C}_2 = \dots\{\rho, C_2\} + v[C_3 \sim C_2 \otimes C_2]$$

Standard RPA: ground state: Slater; ( $C_2 = 0$ )

$$S^0 \chi^0 = \Omega^0 \mathcal{N} \chi^0$$

Inclusion of  $C_2$ :  $\rightarrow$  Second RPA: ground state: CCD

$$\begin{pmatrix} S & B \\ B^+ & D \end{pmatrix} \begin{pmatrix} \chi_1 \\ \chi_2 \end{pmatrix} = \Omega \begin{pmatrix} \mathcal{N} & \mathcal{T} \\ \mathcal{T}^+ & \mathcal{N}_2 \end{pmatrix} \begin{pmatrix} \chi_1 \\ \chi_2 \end{pmatrix} \quad (1)$$

Self-Consistent RPA:

$$S[\chi_1] \chi_1 = \Omega \mathcal{N} \chi_1$$

SCRPA: all properties like RPA! Goldstone, Ward identities, etc  
Kadanoff-Baym  $\rightarrow$  dead end! Too complicated!!

**THANK YOU !**